# Electrochemical Properties of VPO$_4$/C Nanosheets and Microspheres As Anode Materials for Lithium-Ion Batteries

Jun-chao Zheng,[†] Ya-dong Han,[†] Bao Zhang,* Chao Shen, Lei Ming, Xing Ou, and Jia-feng Zhang

School of Metallurgy and Environment, Central South University, Changsha 410083, P. R. China

Ⓢ *Supporting Information*

ABSTRACT: VPO$_4$/C nanosheets and microspheres are successfully synthesized via a hydrothermal method followed by calcinations. The XRD results reveal that the obtained products both have an orthorhombic VPO$_4$ phase. The SEM and TEM images demonstrate that nanosheets and spherical morphology can be obtained by controlling the synthesis conditions. The samples are both uniformly coated by amorphous carbon. The electrochemical test results show that the sample with a nanosheet structure has a better electrochemical performance than the microsphere samples. The VPO$_4$/C nanosheets can deliver an initial discharge capacity of 788.7 mAh g^{-1} at 0.05 C and possessed a favorable capacity at the rates of 1, 2, and 4 C. The nanosheet structure can effectively improve the electrochemical performances of VPO$_4$/C anode materials.
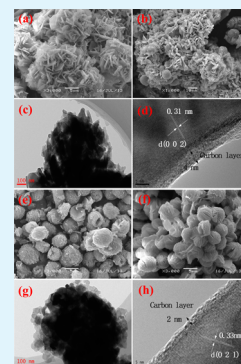
KEYWORDS: *lithium-ion battery, anode material, vanadium phosphate, nanosheet, microsphere*

To meet the growing energy demands for a variety of mobile devices, the development of long-life, low-cost, and high-performance rechargeable lithium-ion batteries has become the trend in today's research.[1−4] The anode material is a critical component of lithium-ion batteries, and the main commercial application is graphite anode. Despite the low cost and good safety of graphite-based anode materials, their relatively low theoretical capacity (372 mAh g^{-1}) and low power density greatly limit their application to match the development of particular high-specific capacity cathode materials.[5−11] Moreover, when metal oxides are used as anode materials, the repeated volumetric change during cycling generates stresses in the electrodes, which results in cracking and fracturing of the active materials and eventually cause the deterioration of the anodes.[9,12] Therefore, developing new anode materials with high specific capacity, low and flat working potential, and long cycle life is of great potential value.

Similar to graphite-based materials, alloys, and metal oxides, three-dimensional phosphate-based polyanionic structures composed of interconnected MO$_6$ octahedra and PO$_4$ tetrahedra can also provide an interstitial space for lithium ion.[6,12−17] The large volume of PO$_4^{3-}$ makes the structure more stable, which alleviates the irreversible changes in volume during the charge and discharge process, which weaken the polarization of electrode materials. The 3D structural framework of MPO$_4$ can supply a fast and smooth lithium-ion pathway, which overcomes the challenge of 1D ion conductivity in olivine.[16] When used as an electrode material, VPO$_4$ provides a high theoretical specific capacity (550 mAh g^{-1}) because of the excellent chemical activity of vanadium (from V to V^{5+}). The reaction mechanism of the VPO$_4$ anode material in lithium-ion batteries is as follows:
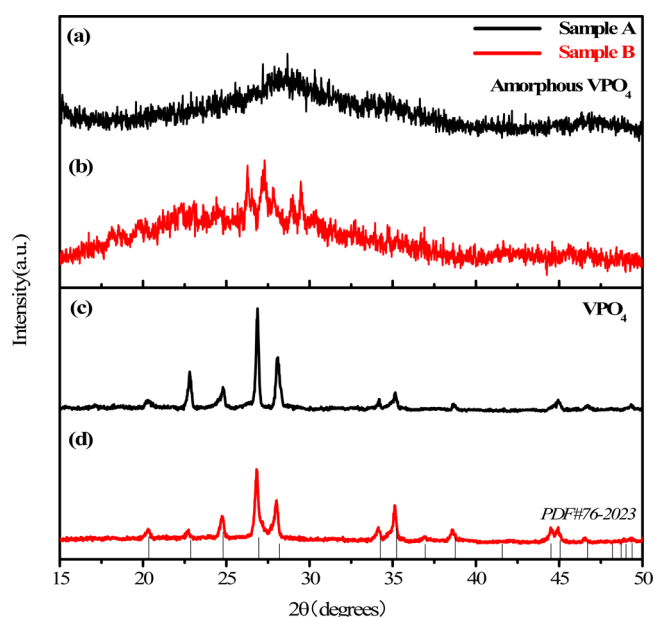

Figure 1. XRD patterns of (a) amorphous V-PO$_4$/C for sample A; (b) amorphous V-PO$_4$/C for sample B; (c) VPO$_4$/C for sample A; (d) VPO$_4$/C for sample B.
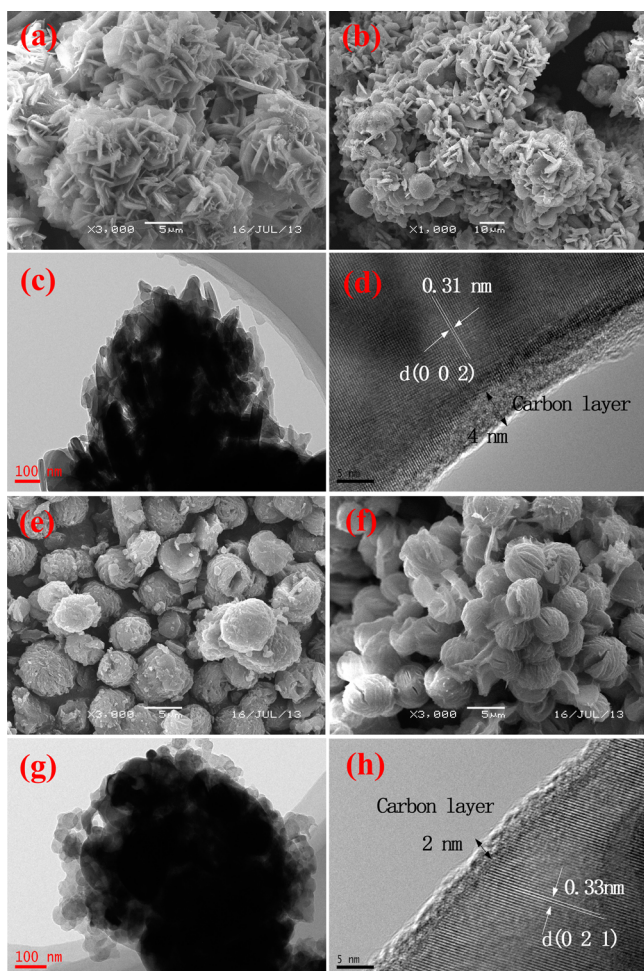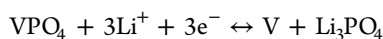
Figure 2. SEM images of (a) amorphous V-PO$_4$/C nanosheet samples and (b) VPO$_4$/C nanosheet samples; (c, d) TEM images of VPO$_4$/C nanosheet samples; SEM images of (e) amorphous V-PO$_4$/C microsphere samples and (f) VPO$_4$/C microsphere samples; (g, h) TEM image of VPO$_4$/C microsphere samples.

$$VPO_4 + 3Li^+ + 3e^- \leftrightarrow V + Li_3PO_4$$

Zhang has proven the feasibility of the use of VPO$_4$ as an anode material via density functional theory (DFT) computations and successfully prepared VPO$_4$/C composite anode materials.[18] However, the use of VPO$_4$ as anode materials for lithium-ion batteries has not been reported yet.

To improve the electrochemical performance of VPO$_4$, nanostructured materials with different morphologies have been synthesized via the hydrothermal method, and their properties are studied in this work.

XRD patterns for samples A and B after hydrothermal treatment are shown in panels a and b in Figure 1. Diffraction peaks were not observed in panels a and b in Figure 1, thereby indicating that the synthesized samples are amorphous. After calcination at a temperature of 725 °C for 4 h, the compound shows a series of diffraction peaks in its XRD pattern, as shown in panels c and d in Figure 1. The samples can be indexed to an orthorhombic structure with the space group *Cmcm* (63), which is in agreement with the peaks at 20.3, 22.8, 24.8, 26.9, 28.2, 34.2, 35.2, 36.9, 38.7, 44.5, and 45.1°, as previously reported.[18,19] No impurities were detected from the patterns, and no additional diffraction peaks related to carbon were observed. However, residual carbons in samples A and B were
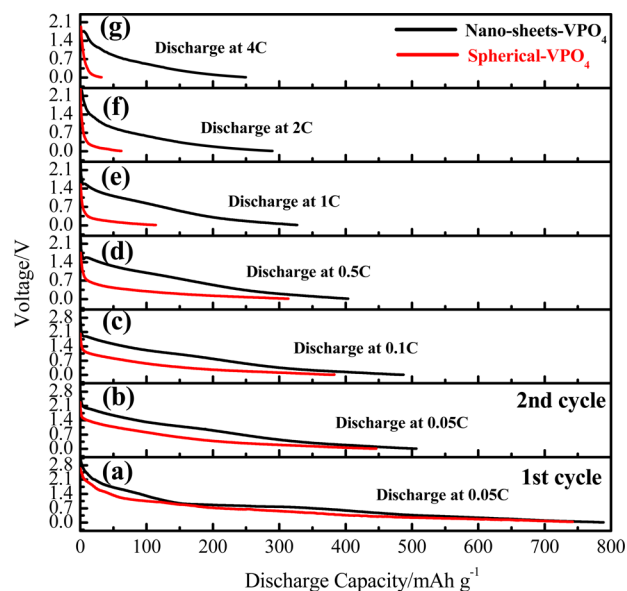

Figure 3. (a−g) Discharge performance of VPO$_4$ nanosheets and microsphere samples at (a) 0.05 *C* for the 1st cycle, (b) 0.05 *C* for the 2nd cycle, and (c) 0.1 *C*, (d) 0.5 *C*, (e) 1 *C*, (f) 2 *C*, and (g) 4 *C*.

both about 3.0 wt % as determined via C−S analysis, thereby indicating that the carbon is amorphous.

Images a and e in Figure 2 are the SEM images of the amorphous V-PO$_4$ precursors for samples A and B, respectively. The amorphous V-PO$_4$ microspheres are composed of nanosheets in sample A (Figure 2a), whereas the structure for sample B is uniform and spherical (Figure 2e). The SEM and TEM images for sample A after calcining the amorphous VPO$_4$ products at 725 °C for 4 h are shown in Figure 2b−d. The primary particles retained the same nanosheet morphology, as shown in images b and c in Figure 2. Staggered nanosheets are uniformly encapsulated in the carbon shell, and the thickness of the carbon shell is about 4 nm, as shown in Figure 2d. The lattice fringe of VPO$_4$ with an interplanar spacing of 0.31 nm corresponds to the (0, 0, 2) lattice planes. Figure 2f−h are the SEM and TEM images of the VPO$_4$ products for sample B. The spherical surface became smooth with some slight agglomeration after calcination. Amorphous carbon was coated on the surfaces with a thickness of about 2 nm, as shown in Figure 2h. Crystal planes with a *d*-spacing of 0.33 nm corresponds to the (0, 2, 1) planes of orthorhombic VPO$_4$.

The discharge behaviors of VPO$_4$/C nanosheets and VPO$_4$/C microspheres anodes are shown in Figure 3a−g between 0.01 and 3.5 V at different rates. From Figure 3a), the initial discharge capacity of VPO$_4$/C nanosheets is 788.7 mAh g^{-1} and that of VPO$_4$/C microspheres is 742.1 mAh g^{-1} at 0.05 *C*, whereas the capacities for the second discharge are 506.5 and 445 mAh g^{-1}, respectively. Given that the theoretical capacity of VPO$_4$ is 550 mAh g^{-1}, the irreversible capacity in the first cycle can be attributed to the reaction of Li ions with oxygen-containing functional groups and the formation of the solid electrolyte interphase (SEI) films.[20−23] No significant difference was observed between the VPO$_4$/C nanosheets and VPO$_4$/C microspheres at the initial discharge. However, at higher rates of 0.1, 0.5, 1, 2, and 4 *C*, the VPO$_4$/C nanosheets are still able to deliver capacities of 487.1, 403.7, 327, 289.6, and 249 mAh g^{-1}, which are higher than those of the VPO$_4$/C microspheres
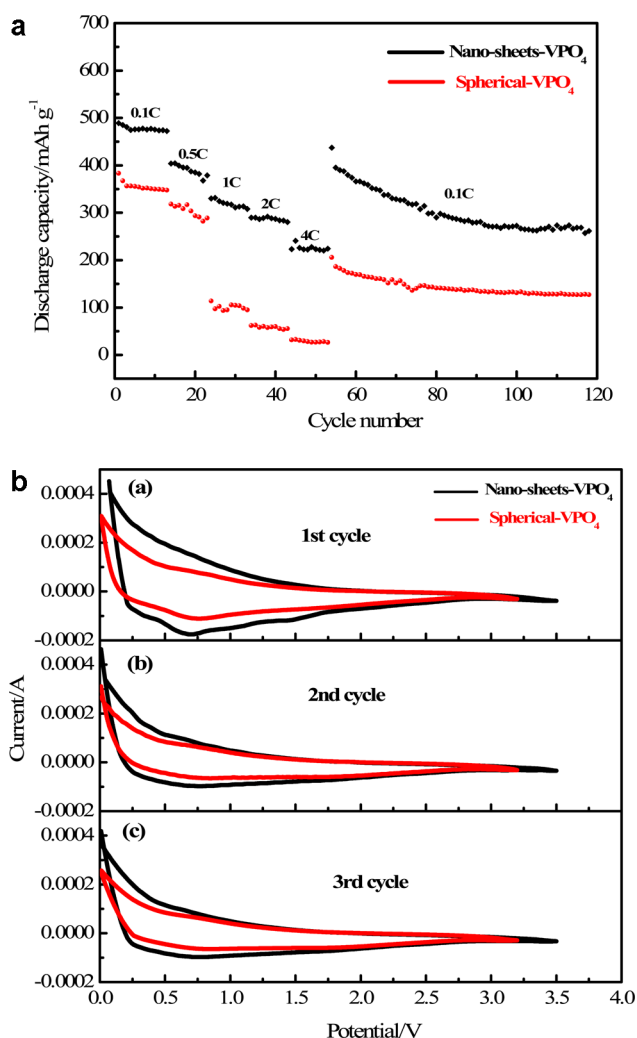
Figure 4. (a) Cycle performance of VPO₄ nanosheets and microsphere samples at 0.1 C, 0.5 C, 1 C, 2 C, and 4 C. (b) (a) 1st, (b) 2nd, (c) 3rd cyclic voltammogram recorded for VPO₄ nanosheets and microsphere samples at a scan rate of 0.1 mV s^{-1}.

at the corresponding rates (382.8, 313.5, 113.7, 62.1, and 32 mAh g^{-1}). The cycle performances are shown in Figure 4a, and the capacity is maintained with increasing cycle and rate. The performances are better that that reported by Zhang, that is, 230.1 mAh g^{-1} after 30 cycles.[18] The reason for this improvement is the special morphology of VPO₄/C and the uniform carbon coating. Comparing the VPO₄/C nanosheets with the VPO₄/C microspheres, the cycle performance of the former is better than that of the latter. The above comparative study shows that the VPO₄/C nanosheets have a much better electrochemical performance than the VPO₄/C microspheres. The excellent electrochemical performance is attributed to the 2D nanosheets structure, which yields stable and thin solid electrolyte interface (SEI) films, produces more sites for lithium ions, possesses larger electrode/electrolyte contact areas, has a shorter diffusion distance, and provides effective transfer pathways for both Li ions and electrons compared with the 3D spherical structure.[10,12,14,24−26] Moreover, the uniform carbon coating can greatly improve the electronic conductivity of the material, which has a great influence on the rate performance of the material.

Figure 4a−c show the initial three-cycle CV profiles of the VPO₄/C nanosheets and VPO₄/C microspheres with a potential range of 0.01 to 3.5 V at a scan rate of 0.1 mV s^{-1}. The oxidation peaks are all located around 0.3 and 0.7 V in the first cycle for both electrodes, which is in agreement with the discharge curves (Figure 3). The oxidation peaks are located at 0.7 V in the second and third cycles. The reason for the difference in the oxidation peaks between the first cycle and the following two cycles indicates the decomposition of the electrolyte and the formation of SEI films during the first cycle.[18] The difference between the two samples is the area bounded by the curves of VPO₄, which corresponds to the energy of the electrode. The area bounded by the curve of VPO₄/C nanosheets is bigger than that of VPO₄/C microspheres, thereby indicating that the discharge capacity of VPO₄/C nanosheets is larger that that of VPO₄/C microspheres, which is consistent with the discharge curves.

In conclusion, VPO₄/C nanosheets and VPO₄/C microspheres were successfully synthesized for the first time via a hydrothermal method followed by calcination. When used as anode electrode materials, both materials showed excellent electrochemical performance because of their unique structure and the uniform carbon coating. The VPO₄/C nanosheets deliver a much higher electrochemical performance than them VPO₄/C microsphere, which can be attributed to the nanosheet structure.

■ ASSOCIATED CONTENT

Ⓢ Supporting Information
Experimental section. This material is available free of charge via the Internet at http://pubs.acs.org.

■ AUTHOR INFORMATION

Corresponding Author
*E-mail: jczheng@csu.edu.cn. Tel:+86-731-88836357.

Author Contributions
†Authors J.Z. and Y.H. contributed equally to this work and should be considered cofirst authors.

Notes
The authors declare no competing financial interest.

■ REFERENCES
(1) Wakihara, M. Recent Developments in Lithium Ion Batteries. *Mater. Sci. Eng., R.* **2001**, *33*, 109−134.
(2) Fergus, J. W. Recent Developments in Cathode Materials for Lithium Ion Batteries. *J. Power Sources* **2010**, *195*, 939−954.
(3) Wang, Y.; Cao, G. Developments in Nanostructured Cathode Materials for High-Performance Lithium-Ion Batteries. *Adv. Mater.* **2008**, *20*, 2251−2269.
(4) Tarascon, J. M.; Armand, M. Issues and Challenges Facing Rechargeable Lithium Batteries. *Nature* **2001**, *414*, 359−367.
(5) Yamaki, J.; Takatsuji, H.; Kawamura, T. Thermal Stability of Graphite Anode with Electrolyte in Lithium-Ion Cells. *Solid State Ionics* **2002**, *148*, 241−245.
(6) Dahn, J. R.; Zheng, T.; Liu, Y. Mechanisms for Lithium Insertion in Carbonaceous Materials. *Science* **1995**, *270*, 590−593.
(7) Persson, K.; Sethuraman, V. A.; Hardwick, L. J. Lithium Diffusion in Graphitic Carbon. *J. Phys. Chem. Lett.* **2010**, *1*, 1176−1180.
(8) Sato, K.; Noguchi, M.; Demachi, A. A Mechanism of Lithium Storage in Disordered Carbons. *Science* **1994**, *264*, 556−558.

(9) Jeong, G.; Kim, Y. U.; Kim, H. Prospective Materials and Applications for Li Secondary Batteries. *Energy Environ. Sci.* **2011**, *4*, 1986−2002.

(10) Ji, L.; Lin, Z.; Alcoutlabi, M. Recent Developments in Nanostructured Anode Materials for Rechargeable Lithium-Ion Batteries. *Energy Environ. Sci.* **2011**, *4*, 2682−2699.

(11) Tarascon, J. M.; Armand, M. Issues and Challenges Facing Rechargeable Lithium Batteries. *Nature* **2001**, *414*, 359−367.

(12) Wu, H. B.; Chen, J. S.; Hng, H. H. Nanostructured Metal Oxide-Based Materials as Advanced Anodes for Lithium-Ion Batteries. *Nanoscale* **2012**, *4*, 2526−2542.

(13) Xue, L.; Fu, Z.; Yao, Y. Three-Dimensional Porous Sn−Cu Alloy Anode for Lithium-Ion Batteries. *Electrochim. Acta* **2010**, *55*, 7310−7314.

(14) Li, H.; Shi, L.; Wang, Q. Nano-Alloy Anode for Lithium Ion Batteries. *Solid State Ionics* **2002**, *148*, 247−258.

(15) Li, H.; Huang, X.; Chen, L. Anodes Based on Oxide Materials for Lithium Rechargeable Batteries. *Solid State Ionics* **1999**, *123*, 189−197.

(16) Sun, C.; Rajasekhara, S.; Dong, Y. Hydrothermal Synthesis and Electrochemical Properties of $Li_3V_2(PO_4)_3$/C-Based Composites for Lithium-Ion Batteries. *ACS Appl. Mater. Interfaces* **2011**, *3*, 3772−3776.

(17) Hautier, G.; Jain, A.; Ong, S. P. Phosphates as Lithium-Ion Battery Cathodes: An Evaluation Based on High-Throughput Ab Initio Calculations. *Chem. Mater.* **2011**, *23*, 3495−3508.

(18) Zhang, Y.; Zhang, X. J.; Tang, Q. Core−Shell VPO_4/C Anode Materials for Li Ion Batteries: Computational Investigation and Sol−Gel Synthesis. *J. Alloys Compd.* **2012**, *522*, 167−171.

(19) Glaum, R.; Reehuis, M.; Stüßer, N. Neutron Diffraction Study of the Nuclear and Magnetic Structure of the $CrVO_4$ Type Phosphates $TiPO_4$ and VPO_4. *J. Solid State Chem.* **1996**, *126*, 15−21.

(20) Liu, H.; Wang, G.; Wang, J. Magnetite/Carbon Core-Shell Nanorods as Anode Materials for Lithium-Ion Batteries. *Electrochem. Commun.* **2008**, *10*, 1879−1882.

(21) Murugan, A. V.; Muraliganth, T.; Manthiram, A. Rapid, Facile Microwave-Solvothermal Synthesis of Graphene Nanosheets and Their Polyaniline Nanocomposites for Energy Strorage. *Chem. Mater.* **2009**, *21*, 5004−5006.

(22) Yoo, E. J.; Kim, J.; Hosono, E. Large Reversible Li Storage of Graphene Nanosheet Families for Use in Rechargeable Lithium Ion Batteries. *Nano Lett.* **2008**, *8*, 2277−2282.

(23) Ota, H.; Sakata, Y.; Inoue, A. Analysis of Vinylene Carbonate Derived SEI Layers on Graphite Anode. *J. Electrochem. Soc.* **2004**, *151*, A1659−A1669.

(24) Hassoun, J.; Panero, S.; Simon, P. High-Rate, Long-Life Ni−Sn Nanostructured Electrodes for Lithium-Ion Batteries. *Adv. Mater.* **2007**, *19*, 1632−1635.

(25) Balaya, P. Size Effects and Nanostructured Materials for Energy Applications. *Energy Environ. Sci.* **2008**, *1*, 645−654.

(26) Jiang, C.; Hosono, E.; Zhou, H. Nanomaterials for Lithium Ion Batteries. *Nano Today* **2006**, *1*, 28−33.